

AIR SPEED CALIBRATIONS AT **THE**
NATIONAL INSTITUTE OF **STANDARDS AND TECHNOLOGY**

N. E. Mease, W. G. Cleveland, Jr., G. E. Mattingly, and J. M. Hall
Fluid Flow Group
Process Measurements Division
Chemical Science and Technology Laboratory
National Institute of Standards and Technology
Gaithersburg, MD 20899

ABSTRACT

The wind tunnel facilities and equipment used for air speed calibrations at the National Institute of Standards and Technology (NIST) are described with details of the tunnels' construction and their performance characteristics. The mathematical relationships for air speed computations are shown and error budgets for both the Pitot-static tube and Laser Doppler anemometer (LDA) measuring systems are discussed. The performance relationships for these two systems and the advantages of each are presented. Examples are given to show the method for accounting for changes in fluid density by including the effects of pressure, temperature, and humidity. A relationship is given for computing air speed from Pitot-static tube measurements, including the effects of compressibility. Random uncertainty analysis for the air speed relationships is discussed and quantified using the NIST conditions. The associated systematic error estimates are discussed in terms of round-robin assessment methods.

INTRODUCTION

The measurement of the movement of air had its beginning at NIST in the very early days of aircraft development. Today, weather, ventilation, and environmental concerns have become equally important fields requiring the quantification of air speed, as air is one of the most common fluids which provides a convective medium for contaminants. These measurements are made using anemometers, which in most cases need to be calibrated against a known air speed. The use of anemometers is not limited to air; measurements can be made in other gases and liquids as well. It is also possible to calibrate an instrument in one fluid and make measurements in another fluid if the response of the instrument to changes in fluid density and kinematic viscosity is understood.

Generally, anemometry, or “point velocity” measurement techniques must be used to quantify the movement of fluids under conditions where bulk flow (mass or volume) measurements cannot be made such as where the flow is unbounded, i.e. in cross-sections that are very large, or where pressure drops produced by other types of instrumentation are unacceptable. Also, wherever flow velocity distributions are required, anemometry must be used. The range of measurement requirements for anemometers may be divided into two regimes depending on instrument application and flow velocity: 1) meteorological or outdoor (high speed), and 2) ventilation or indoor (low speed). NIST has addressed these needs with two facilities employing different measurement techniques.

NIST WIND TUNNEL FACILITIES

In the past the calibration of anemometers has been done in several ways at NIST. The whirling arm and towing tunnel were used at one time. Reference [1] provides some history of other very early facilities. In the early 1970's, two new wind tunnels were built, the NIST Dual Test Section Wind Tunnel (DTSWT) shown in figure 1 and the NIST Low Velocity Facility (LVF) shown in figure 2.

The DTSWT is a closed-circuit facility lying in a horizontal plane. The tunnel is powered by a 370 kW (500 hp) AC-to-DC motor generator set which supplies DC power to a 300 kW (400 hp) drive motor. The maximum drive rpm is 600 and is controlled by a feedback loop producing shaft revolutions stable to within ~0.1%. The drive motor turns a 2.4 m (8 ft) two-stage axial flow fan with manually adjustable blade pitch. Downstream of the fan the flow passes through a circular-to-square transition section and into a five-degree diffuser. The diffuser continues around through two sets of turning vanes, through a 3.7 m (12 ft) square cross-section containing a 1 cm by 7.6 cm (3/8 in by 3 in) phenolic resin honeycomb and then into a wide-angle diffuser [2]. The wide-angle diffuser contains 6 screens and discharges into a 6.2 m by 7.6 m (20 ft, 2 in by 25 ft) settling chamber containing 9 screens. All screens are 20 mesh stainless steel made with 0.023 cm (0.009 in) diameter wire, and are spaced 0.61 m (2 ft) apart in the flow direction. From the settling chamber the flow passes through an entrance cone and into a 1.5 m by 2.1 m (5 ft by 7 ft) cross-section where folding hinges are attached to facilitate changing test sections. The honeycomb, screens, and a contraction ratio of 14.4-to-1 provide test section longitudinal free-stream turbulence levels of 0.07% over most of the speed range and a transverse velocity gradient within a 90% “working window” of less than 1% in both test sections.

The test section assembly consists of two ducts which ride “piggy back” on a cable hoisting arrangement. The upper test section is 12 meters (39 ft, 7 in) long and has a system of parallel arms along the sides which allow the sidewalls to be adjusted to provide a zero pressure gradient for research purposes. This test section is variable in cross-section but nominally measures 2.1 m (7 ft) high and 1.5 m (5 ft) wide with the 1.5 m width variable. The top speed in the 2.1 m by 1.5 m configuration is about 45 m/s

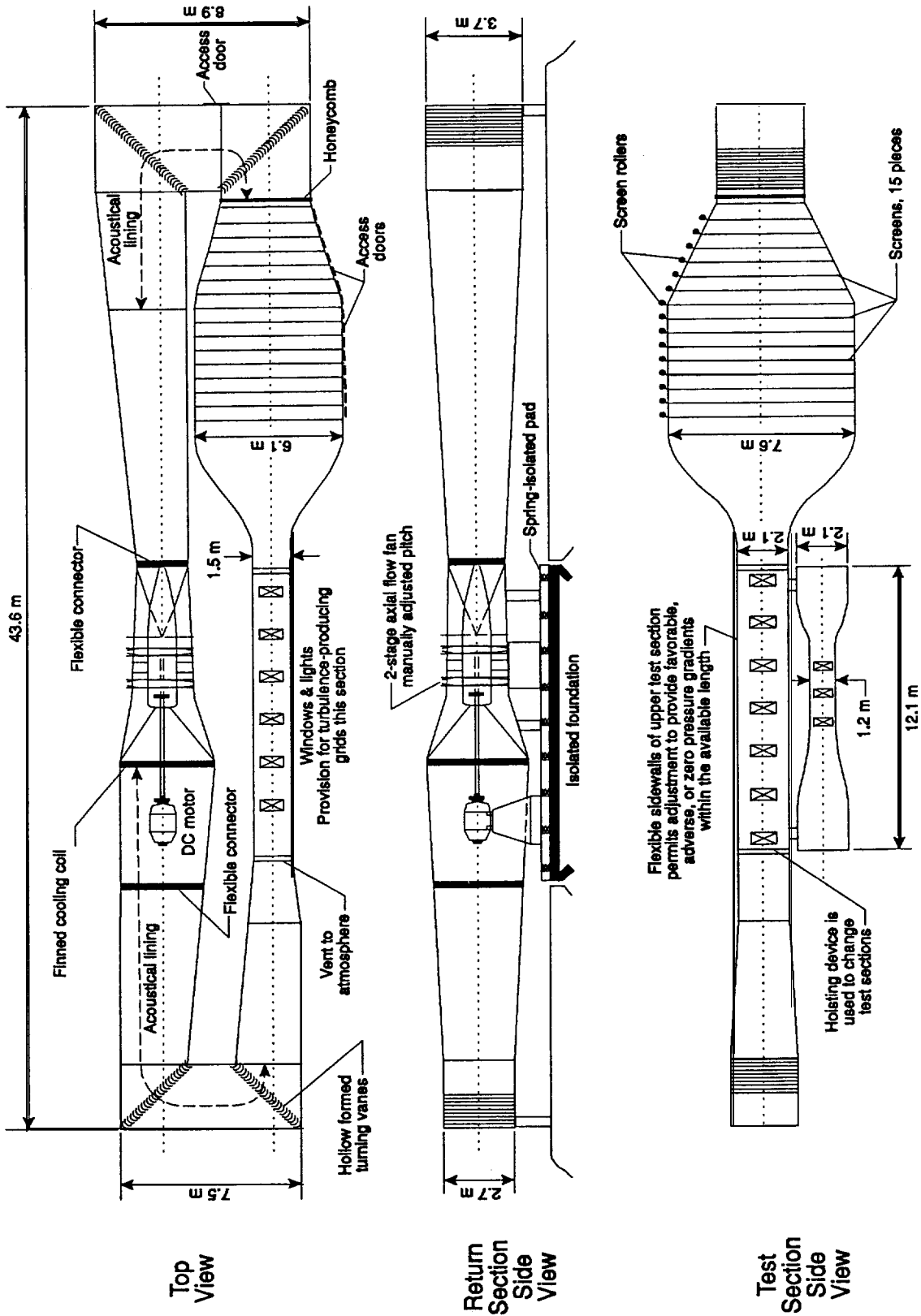


Figure 1. NIST Dual Test Section Wind Tunnel (DTSWT).

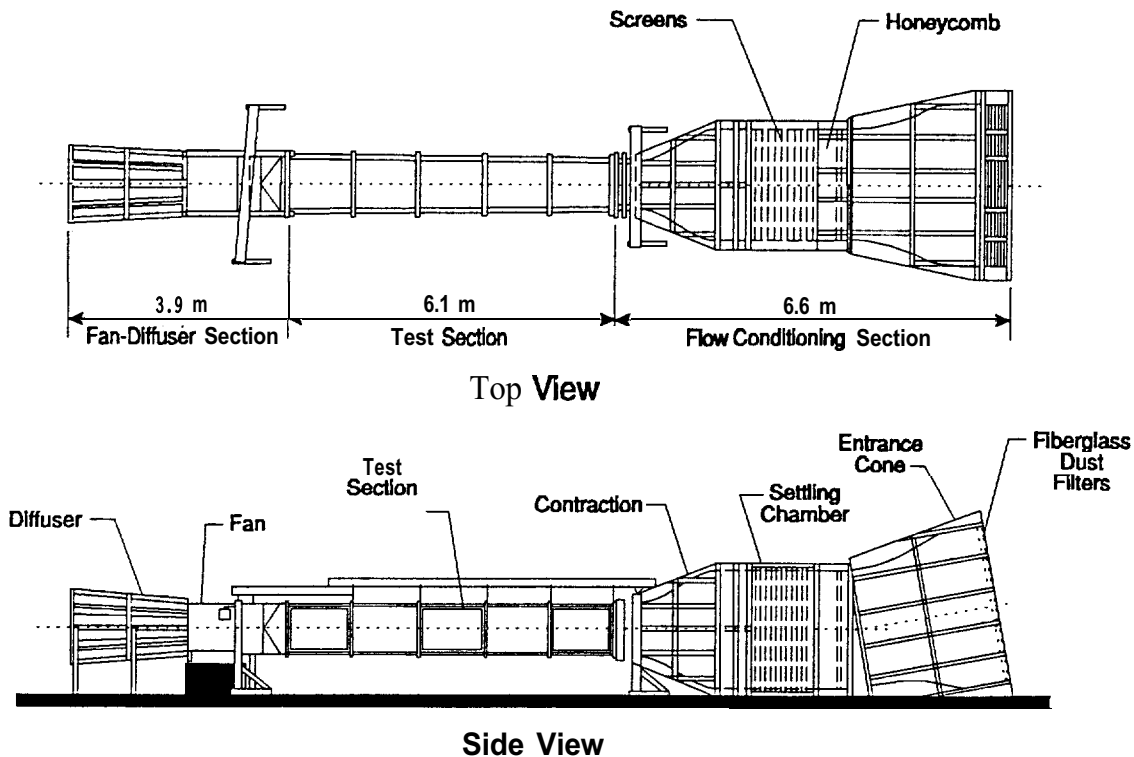


Figure 2. NZST Low Velocity Facility (LVF).

(100 mph). The 2.1 m vertical dimension at the entrance to the lower test section is gradually reduced in the flow direction to 1.2 m (4 ft) forming a venturi-like duct so that the top speed is about 67 m/s (150 mph). The effective working length is 3.0 m (10 ft) within the overall 12.1 m length. All sides of the lower test section are fixed. Both test sections are equipped with overhead lighting and windows in the sidewalls for observation and access. The entire assembly has a mass of about 1.8×10^4 kg (20 tons).

The downstream end of the test sections is vented to room air establishing this point in the closed-circuit system as being near atmospheric pressure and temperature conditions. From this point the flow passes into a five-degree diffuser, around two 90-degree bends containing turning vanes and into the drive section which measures 3.8 m by 4.37 m (12 ft, 5 in wide by 14 ft high) at the location of a cooling coil used to stabilize the tunnel temperature. The cooling coil is situated between the drive motor and the fan and a 15 cm (6 in) drive shaft passes through the center of the coil. A rectangular to 2.4 m (8 ft) round transition completes the circuit connection to the drive fan inlet. The entire drive mechanism, along with the cooling coil, is mounted on a large concrete slab which is isolated from the building floor with springs to minimize the transmission of vibration. The main tunnel duct is attached to the drive section at each end by means of flexible boots.

The LVF, shown schematically in figure 2, is described in detail in reference [3]. The

test section is fabricated of transparent acrylic plastic sheet supported by steel framing. The top speed is about 11.2 m/s (2200 fpm). Recently, the tunnel was upgraded by replacing the drive with a system similar to that of the DTSWT, including the addition of remotely controlled variable-pitch fan blades. Additional improvements have been made to the air speed measuring system and will be discussed later.

PRIMARY AIR SPEED MEASUREMENT SYSTEMS

The Pitot-static Tube In the DTSWT the air speed measurement system currently in use consists of measuring the differential pressure produced between the total and static pressure ports of an adopted laboratory standard Pitot-static tube. The air speed may be determined using Bernoulli's Law in its usual form, which is

$$V_i = \left[\frac{2 (P_o - P_s)}{\rho} \right]^{1/2}, \quad (1)$$

where, in compatible units, V_i is the computed air speed for an air flow assumed to be incompressible, $(P_o - P_s)$ is the difference between the total pressure, P_o , and static pressure, P_s , in the air flow and ρ is the density of the air. Assuming the real gas law,

$$P_o = \frac{\rho}{M} Z R T_o, \quad (2)$$

is valid for the specific flow conditions, eq (1) may be written

$$V_i = \left[\frac{2 Z R T_o (P_o - P_s)}{M P_o} \right]^{1/2} \quad (3)$$

where R is the universal gas constant, M is the molecular weight of the gas, and T_o is the temperature of the gas. Z is a non-dimensional factor that is used to account for the **non-ideality** of gas mixtures and varies slightly with pressure, temperature, and relative humidity. Values of Z for air are available in tabulated form in reference [4].

As a result of a NIST study (unpublished) of the nose shapes of Pitot-static tubes performed in the late 1960's, the laboratory standard Pitot-static tube used at NIST was changed from a hemispherical-nose type to a **6-to-1** modified ellipsoidal-nose design [5]. In the study, several ellipsoidal-nosed tubes were fabricated at NIST and intercomparisons were made to see if the presence of the total pressure port affected the static pressure indication. No effect was found. These tubes were also compared to the hemispherical-nosed design, and to tubes with other nose shapes including conical and a **4-to-1** modified ellipsoidal shape. It was found that the static pressure indications of the hemispherical-nosed tube changed at about 71.5 m/s (160 mph) due to the transition

region from laminar to turbulent flow moving forward on the tube and getting closer to the static pressure ports. This was not observed on the **6-to-1** modified ellipsoidal-nosed tube as the transition region always remained sufficiently far downstream at speeds up to 76 m/s as to not influence the indicated static pressure. The difference is believed to be due to the lower pressure gradient - a parameter known to strongly affect the position of the transition region - around the curvature of the 6-to-1 ellipsoidal nose.

Most published constants for M and ρ are for dry air, seldom found in wind tunnel environments, so it is necessary to account for the moisture content of the air. Relative humidity decreases the density in eq (2) and, therefore, the value of M must also decrease for the same values of P_o and T_o . In other words, moist air is lighter than dry air, contrary to the intuition of most people. The density or the apparent molecular weight of moist air may be calculated using the analysis of Jones [6]:

$$\frac{\rho_h}{\rho_d} = \frac{M_h}{M_d} = 1 + \frac{(\epsilon - 1) e'}{P_o}, \quad (4)$$

where ρ_h is the density of the moist air, ρ_d is the density of dry air, M_d and M_h are the apparent molecular weights of dry and humid air, respectively, ϵ is the ratio of the molecular weight of water to the molecular weight of dry air (0.62201), and e' is the relative humidity in percent divided by 100 and multiplied by the saturation vapor pressure of water vapor, which is available in any steam table [7]. Using eq (4), values of ρ_h , or M_h , may be determined from constants for dry air and used in air speed calculations. The value of M_d for dry air is 28.963 and the value of R is 8.3148 JK⁻¹/mol [5]. Care must be taken in the use of some reference values of R as they are actually R/M as herein defined. For example, reference [8] gives a value for air of "1716.322 ft²/(sec² °R)" for "gas constant"; this value is equal to the universal gas constant divided by the molecular weight of air.

Table 1 shows the effect of relative humidity on the air density and calculated air speed for typical conditions, $P_o = 101 \text{ kPa}$ (760 mm Hg) and $T_o = 20 \text{ °C}$, prevailing in the NIST wind tunnels at an air speed of about 20 m/s. The percentage differences shown in the table have been computed relative to the dry air condition which is given on the first line. It must be noted that if the effect of relative humidity is neglected in air speed measurements made with Pitot-static tubes, sufficient allowance must be included in the systematic error estimate of the measurement.

In order to include possible compressibility effects in the air stream, the "Compressible Bernoulli Equation" is used at NIST in a modified form [9]. This equation assumes that the flowing gas is thermally perfect and that the flow acceleration process is isentropic, which are both valid assumptions for low speed air flows. The compressible equation of reference [9], when solved for velocity, V_o , can be written

Table 1. Effect of Relative Humidity on Air Density and Air Speed				
Relative Humidity, %	Air Density kg/m ³	Difference %	Air Speed m/s	Difference %
0	1.1924	0	19.971	0
10	1.1915	0.075	19.798	0.035
20	1.1906	0.15	19.806	0.076
30	1.1896	0.23	19.814	0.12
40	1.1884	0.34	19.824	0.17
50	1.1871	0.44	19.835	0.22
60	1.1856	0.56	19.847	0.28
70	1.1839	0.71	19.861	0.35
80	1.1820	0.87	19.877	0.43
90	1.1799	1.00	19.895	0.53

$$V_c = \left[\frac{2\gamma}{\gamma-1} \left(\frac{P_o}{\rho_o} \right) \right]^{1/2} \left[\left(1 - \frac{P_s}{P_o} \right)^{\frac{\gamma-1}{\gamma}} \right]^{1/2}, \quad (5)$$

where γ is the ratio of the specific heats (1.4 for air), P_o and P_s are as defined above and ρ_o is the density that the moving air would have at stagnation conditions, i.e. at zero speed. It can be seen that this relationship does not contain the term $(P_o - P_s)$, the pressure difference measured directly with a Pitot-static tube. By again employing the real gas law, eq (2), and by adding and subtracting P_o from the right-hand side of eq (5), the relationship can be rewritten

$$V_c = \left[\frac{2\gamma ZRT_o}{(\gamma-1) M_h} \right]^{1/2} \left[1 - \left(1 - \frac{(P_o - P_s)}{P_o} \right)^{\frac{\gamma-1}{\gamma}} \right]^{1/2}, \quad (6)$$

which now contains the quantity $(P_o - P_s)$ and is as convenient to use as the incompressible relationship, eq (3). It is important that the temperature used in eq (5) be the measured stagnation temperature, T_o . Equation (6) is the relationship used at NIST for calculating air speeds from Pitot-static tube differential pressure measurements. It should be noted that the underlying assumptions of eq (6) are invalid across a shock and should be carefully considered if the Mach number approaches unity. Also, if

compressibility is neglected in making air speed computations, the corresponding error analysis must include an allowance for this effect as being systematic.

Pitot-static tube measuring systems are inexpensive, easy to construct, assemble, and use with knowledge of basic fluid flow principles. They can be mounted in inaccessible locations and measurements made remotely with no optical access requirements. The non-linear nature of Bernoulli's Law can produce large errors as the speed decreases, limiting the system's use at low speeds. Non-steady flows can cause bias in air speed measurements not only due to the non-linear nature of the system but also because the total and static pressure signals in any given system may have different response times.

Laser Doppler Anemometry

The LVF uses Laser Doppler anemometry (LDA) as the primary measurement system, along with Pitot-static tube techniques as described in [3]. The air speed in an LDA system is determined from the measured period of scattered light produced by a small particle passing through the fringes in the intersection volume of two Laser beams by using the relationship

$$V = L / \tau , \quad (7)$$

where V is the particle speed and τ is the average period between fringes, as determined by the Laser processor, of the scattered light produced by the particle passing through the intersection volume of the Laser beams. The length L contains parameters that are **fixed** constants and are characteristic of a particular LDA system (changing only slightly from day to day due to temperature gradients in the optics) and can be expressed as

$$L = \frac{\lambda}{2 \sin (\theta/2)} , \quad (8)$$

where λ is the wave length of the Laser light and θ is the angle between the two Laser beams. The original LDA system at NIST described in reference [3] was a prototype which has been upgraded with the addition of an automated data acquisition computer, commercially available LDA processor, and improved beam splitter optics. Figure 3 is a schematic diagram of the LDA optical system. Not shown are the processor, which determines the average period, τ , of the scattered light from the photomultiplier tube (PMT) signal, and the computer system.

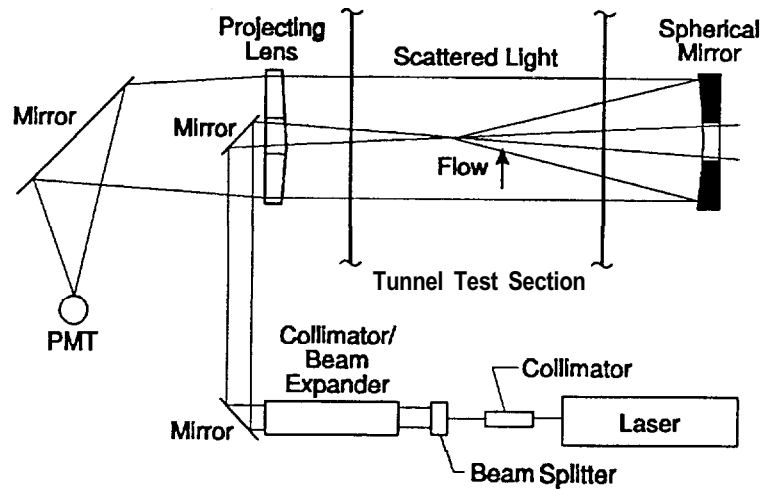


Figure 3. LDA optical system used in NISLVF.

The major attributes of an LDA system are its linear performance relationship, independence from fluid properties, and the fact that it is non-intrusive to the flow. However, it is expensive and requires highly skilled personnel for continuous reliable operation. In addition, associated optical systems may need to be specifically designed for each application in order to obtain greatest sensitivity, and particle seeding of the flow is often required to obtain reasonable data rates.

ERROR ANALYSIS

Random Errors At NIST Pitot-static tube differential pressures are measured using a sloping manometer so that

$$(P_o - P_s) = \rho_m g_l l \sin \alpha \quad , \quad (9)$$

where ρ_m is the density of the manometric fluid, g_l is the local acceleration of gravity, α is the angle between the fluid column and the horizontal, and l is the manometer reading. Substituting eq (9) into eq (2), and substituting M_h for M , the result obtained is

$$V_i = \left[\frac{2\rho_m g_l l Z R T_o \sin \alpha}{M_h P_o} \right]^{1/2} . \quad (10)$$

Because of its simplicity, it is preferable to use eq (10) instead of eq (6) to make random error estimates. The difference is in neglecting terms containing γ , a well-documented constant that will make an insignificant random error contribution. The error due to neglecting terms containing γ can be included in an over-all allowance for possible systematic error as mentioned previously.

Reference [10] discusses error analysis for the NIST air speed measuring systems. Instead of summing the error components in quadrature, the absolute values are summed, since there is a possibility that some of the individual error components may be correlated. The resulting error estimate will be for a worst-case condition. Summing all component values, except A/l , for the instrumentation used in the DTSWT gives

$$\text{Error in } \frac{\Delta V}{V} \leq \frac{1}{2} \left(\frac{\Delta l}{l} \right) + .0012 . \quad (11)$$

At the highest speeds of the DTSWT, the value of A/l is about 0.0001, which gives a value of 0.0013 using eq (11). For a 99% confidence interval (3σ level, where σ is the standard deviation), plus an allowance of 0.0001 for possible systematic error, an overall error estimate of $\pm 0.4\%$ is obtained for the higher speeds of the DTSWT. As the speed decreases, the value of $\Delta l/l$ in eq (11) gradually becomes larger and more significant beginning at about 10 m/s. The best estimate of total uncertainty for the speed range available in the DTSWT is shown in figure 4.

If the expression for L of eq (8) is substituted into eq (7) and an error analysis is performed similar to the Pitot-static tube analysis above, it is seen that the major error contribution comes from the $\sin(\theta/2)$ term. In the LVF all parameters, except τ , are grouped together as shown in eq (8). The quantity L is then determined by measuring the air speed, using the Pitot-static tube system with the tunnel air speed set at about 10 m/s, and then solving eq (7). The quantity L varies very little and changes primarily with temperature, as previously stated, due to

seasonal changes. Since the Pitot-static system is also available in the tunnel, this method avoids the need to determine $\sin(\theta/2)$ using additional measurement techniques. Using this method, the LDA system is calibrated against the Pitot-static tube system at a speed sufficiently high that the Pitot-static tube velocity uncertainty is less than the requirements for the LDA system uncertainty. The LDA processor and computer system determine values of τ and compute a running mean and standard deviation which is updated as each new velocity determination is added. To estimate the error for the LDA system, the uncertainty estimate of 0.4% determined for the Pitot-static tube system must be considered as possible systematic error. The standard errors for the calibration measurement of τ both for the determination of L and the actual measured velocity may be calculated and added in quadrature. About 315 data points are averaged for both and each has a standard deviation of about 2.5%. For a 99% confidence interval of the mean, the total uncertainty, U , of the mean air speed measured in the LVF will be

$$U = 0.4\% + 3 \left[\left(\frac{2.5\%}{\sqrt{315}} \right)^2 + \left(\frac{2.5\%}{\sqrt{315}} \right)^2 \right]^{1/2}, \quad (12)$$

or about 1% as shown in figure 4. Since the system is linear, the uncertainty will be a constant over the entire speed range making the LDA system greatly superior to the Pitot-static tube system for low speed measurements.

Systematic Error To properly quantify the systematic error of a measurement system, its results must be compared to other similar systems using appropriate transfer standards. In rate measurements such as air speed and fluid flow systems, this is conventionally done using round-robin techniques which have shown that allowances for systematic error

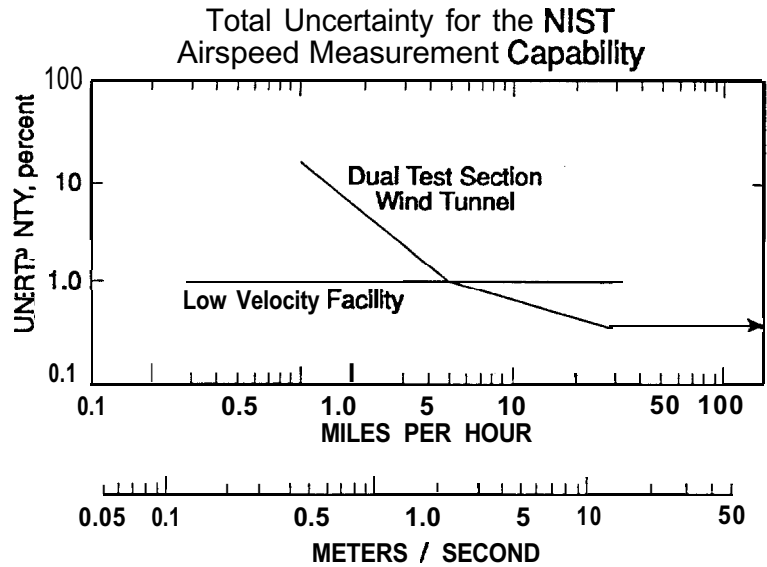


Figure 4. NIST air speed calibration uncertainty.

may be low by as much as a factor of five [11-14]. The only round-robin testing results which have been reported to date for air speed measurements are those of Lockhart [15]. In this test, a propeller anemometer having an estimated true blade pitch of 0.2963 meters per revolution, m/r, was used. The NIST measured value was 0.2967 m/r. The mean of 18 different calibration laboratory determinations was 0.2965 m/r indicating very close agreement to the measured NIST value. The difference between the NIST value and the mean is 0.067%, indicating that the allowance of 0.1% for possible systematic error used in the previous error discussion of the Pitot-static tube system is reasonable.

Recently, a need has been defined by members of the Biomedical and Pharmaceutical Metrology Committee of the National Conference of Standards Laboratories (NCSL), with additional interest indicated by the American Society of Heating, Refrigerating and Air-Conditioning Engineers (ASHRAE), to perform a round-robin test in the air speed range of 0.5 to 25 m/s (100 to 5,000 fpm), a speed range of interest in all fields concerned with indoor ventilation. The wind tunnels at NIST will be used in this testing program.

ACKNOWLEDGEMENT

The air speed calibration service at NIST has been an evolving activity driven by the needs of its many customers. Therefore, the authors wish to thank these customers for their contribution to the continued development of this important area of the national measurement system.

REFERENCES

1. Cochrane, Rexmond C., Measures for Progress. A History of the National Bureau of Standards, Nat. Bur. Stand., Washington, DC, (1966).
2. Schubauer, G. B., and Spangenberg, W. G., "Effect of Screens in Wide Angle Diffusers", NACA Report 949, (1949).
3. Pm-tell, L. P., and Klebanoff, P. S., "A Low-Velocity **Airflow** Calibration and Research Facility", Nat. Bur. Stand., NBS Technical Note 989, (1979).
4. List, R. J., Smithsonian Meteorological Tables, 6th rev. ed., The Smithsonian Institution, Washington, DC, (1951).
5. Salter, C., Warsap, J. H., Goodman, D. G., "A New Design of Pitot-static Tube with a Discussion of Pitot-static Tubes and Their Calibration Factors", Nat. Phys. Lab. (U.K.), NPL Aero. Report 1013, (1962).

6. Jones, F., 'The Air Density Equation and Transfer of the Mass Unit', J. Res. Nat. Bur. Stand. (U. S.), Vol. 83, No. 5, (1978).
7. Haar, L., Gallagher, J. S., Kell, G. S., NBS/NRC Steam Tables. Thermodynamic and Transport Properties and Computer Programs for Vapor and Liquid States of Water in SI Units, Hemisphere Publishing Corp., New York, NY, (1984).
8. The Aerodynamics Handbook Staff of The Johns Hopkins Applied Physics Laboratory, "Handbook of Supersonic Aerodynamics", NAVORD Report 1488, Vol. 2, (1950).
9. Ames Research Staff, "Equations, Tables and Charts for Compressible Flow", NACA Report 1135, (1953).
10. Mattingly, G. E., Mease, N.E., "Gas Flow Measurement: Practical Aspects and Research Results", IGT Symposium on Natural Gas Energy Measurement, Chicago, IL, (1988).
11. Mattingly, G. E., "Dynamic **Traceability** of Flow Measurements", IMEKO Symposium on Flow Measurement and Control in Industry, SICE, Tokyo, Japan, (1979).
12. Mattingly, G. E., "Primary Calibrators, Reference and Transfer Standards", Developments in Flow Measurement, Chap. 2, Applied Science, Englewood, NJ, (1982).
13. Mattingly, G. E., "Volume Flow Measurements", Fluid Mechanics Measurements, Chap. 6, Hemisphere Publishing Corp., New York, NY, (1983).
14. Mattingly, G. E., "A Round Robin Flow Measurement Testing Program Using Hydrocarbon Liquids: Results for First Phase Testing", Nat. Inst. of Standards and Technol., NISTIR 88-4013, (1988).
15. Lockhart, T. J., "Relative Accuracy of Wind Tunnel Calibration Speeds", Preprints of the Amer. Metrological Soc. 7th Symp. on Observations and Measurements, New Orleans, LA, (1991).